Molecular Biology of the Cell
Vol. 21, 1214–1224, April 1, 2010

Par-4: A New Activator of Myosin Phosphatase

Susanne Vetterkind,* Eunhee Lee,† Eric Sundberg,† Ransom H. Poythress,* Terence C. Tao,† Ute Preuss,‡ and Kathleen G. Morgan*

*Department of Health Sciences, Sargent College of Health and Rehabilitation Sciences, Boston University, Boston, MA 02215; †Boston Biomedical Research Institute, Watertown, MA 02472; and ‡Institute of Genetics, University of Bonn, D-53117 Bonn, Germany

Submitted August 19, 2009; Revised January 21, 2010; Accepted January 26, 2010
Monitoring Editor: Mark H. Ginsberg

Myosin phosphatase (MP) is a key regulator of myosin light chain (LC20) phosphorylation, a process essential for motility, apoptosis, and smooth muscle contractility. Although MP inhibition is well studied, little is known about MP activation. We have recently demonstrated that prostate apoptosis response (Par)-4 modulates vascular smooth muscle contractility. Here, we test the hypothesis that Par-4 regulates MP activity directly. We show, by proximity ligation assays, surface plasmon resonance and coimmunoprecipitation, that Par-4 interacts with the targeting subunit of MP, MYPT1. Binding is mediated by the leucine zippers of MYPT1 and Par-4 and reduced by Par-4 phosphorylation. Overexpression of Par-4 leads to increased phosphatase activity of immunoprecipitated MP, whereas small interfering RNA knockdown of endogenous Par-4 significantly decreases MP activity and increases MYPT1 phosphorylation. LC20 phosphorylation assays demonstrate that overexpression of Par-4 reduces LC20 phosphorylation. In contrast, a phosphorylation site mutant, but not wild-type Par-4, interferes with zipper-interacting protein kinase (ZIPK)-mediated MP inhibition. We conclude from our results Par-4 operates through a "padlock" model in which binding of Par-4 to MYPT1 activates MP by blocking access to the inhibitory phosphorylation sites, and inhibitory phosphorylation of MYPT1 by ZIPK requires "unlocking" of Par-4 by phosphorylation and displacement of Par-4 from the MP complex.

INTRODUCTION

Smooth muscle and nonmuscle myosin activity, required for numerous cellular processes such as motility, mitosis, apoptosis, and smooth muscle contractility, is regulated by the phosphorylation state of the myosin regulatory light chain (LC20) at serine 19. LC20 phosphorylation, in turn, is determined by the opposing activities of myosin light chain kinase (MLCK) and myosin phosphatase. The smooth muscle myosin phosphatase holoenzyme (MP) is a heterotrimeric protein complex composed of the catalytic subunit PP1cδ, the regulatory/targeting subunit MYPT1, and a small subunit of largely unknown function (for a review, see Ito *et al*., 2004). MYPT1 has a central role in the function of MP: The 110-kDa protein acts as a targeting subunit, directing PP1cδ to its substrate LC20 (Shimizu *et al*., 1994). Furthermore, MYPT1 enhances the catalytic activity of PP1cδ toward LC20 (Alessi *et al*., 1992; Shirazi *et al*., 1994). Moreover, MYPT1 possesses two inhibitory phosphorylation sites, threonine 696 and threonine 853 (mammalian numbering), which, upon phosphorylation, lead to inhibition of the MP holoenzyme (Kimura *et al*., 1996; Feng *et al*., 1999). The two inhibitory phosphorylation sites are located in the C-terminal part of MYPT1, which also harbors binding sites for myosin, phospholipids, RhoA, the type Ia cGMP-dependent protein kinase (PKG), and the small subunit of MP (Ito *et al*., 2004). Binding of MYPT1 to PP1cδ and phosphorylated LC20 is mediated by an ankyrin repeat region in the N-terminal part of the protein (Ito *et al*., 2004). Alternative splicing gives rise to four major isoforms of MYPT1 that differ in the presence of a central insert and/or a C-terminal leucine zipper motif (Chen *et al*., 1994; Dirksen *et al*., 2000).

The best defined signaling pathway that leads to inhibitory phosphorylation of MYPT1 is the Rho/Rho kinase pathway: lysophosphatidic acid (LPA) binding to a G protein-coupled receptor mediates activation of the small GTPase Rho (Ridley and Hall, 1992). Activated Rho then binds to, and activates Rho kinase (Matsui *et al*., 1996), which in turn phosphorylates MYPT1 and inhibits MP (Kimura *et al*., 1996). Apart from Rho kinase, inhibitory phosphorylation of MYPT1 can be performed by integrin linked kinase (ILK) (Kiss *et al*., 2002; Muranyi *et al*., 2002) and by zipper-interacting protein kinase (ZIPK) (MacDonald *et al*., 2001; Endo *et al*., 2004), another substrate of Rho kinase (Hagerty *et al*., 2007).

In contrast, MP activation, which is primarily reported to be mediated by the nitric oxide (NO) pathway, is less well understood. The activating effect of NO on MP is primarily mediated by PKG (Nakamura *et al*., 1999; Surks *et al*., 1999; Wooldridge *et al*., 2004). However, there are some discrepancies about the nature of the PKG–MYPT1 interaction (Surks *et al*., 1999; Khatri *et al*., 2001; Surks and Mendelsohn, 2003; Huang *et al*., 2004; Given *et al*., 2007; Lee *et al*., 2007; Sharma *et al*., 2008), and whether phosphorylation of MYPT1 by PKG is involved in activation of MP (Nakamura *et al*., 1999; Wooldridge *et al*., 2004) has yet to be fully resolved.

Prostate apoptosis response (Par)-4 is a proapoptotic protein with multiple functions (Sells 1994, Diaz-Meco *et al*., 1996). In nonmuscle cells, Par-4 induces apoptosis in at least three ways: 1) by acting as a transcriptional regulator (Johnstone *et al*.,

This article was published online ahead of print in *MBoC in Press* (http://www.molbiolcell.org/cgi/doi/10.1091/mbc.E09–08–0711) on February 3, 2010.

Address correspondence to: Kathleen G. Morgan (kmorgan@bu.edu).

Abbreviations used: LC20, myosin light chain; LPA, lysophosphatidic acid; MP, myosin phosphatase; NO, nitric oxide; Par, prostate apoptosis response; ZIPK, zipper-interacting protein kinase.

1996; Richard *et al*., 2001; Cheema *et al*., 2003; Lu *et al*., 2008); 2) by inhibiting the prosurvival kinases atypical protein kinase C (aPKC)ζ (Diaz-Meco *et al*., 1996; Leroy *et al*., 2005; Wang *et al*., 2005) and protein kinase B (PKB)/Akt (Joshi *et al*., 2008; Lee *et al*., 2008); or 3) by interacting with ZIPK (Page *et al*., 1999; Kawai *et al*., 2003), accompanied by changes in LC20 phosphorylation (Vetterkind *et al*., 2005b). We have recently reported that Par-4 has a nonapoptotic function in regulating smooth muscle contractility by targeting ZIPK to actomyosin filaments during agonist activation (Vetterkind and Morgan, 2009). Using recombinant proteins and a cell culture model for smooth muscle cells, we now pursue the mechanism of Par-4 function and demonstrate that phosphorylation of Par-4 is required for ZIPK-mediated inhibition of MYPT1 after agonist stimulation. Moreover, we show, for the first time, that in the absence of agonists, Par-4 directly binds to and activates MP. We propose a model, consistent with these data, where Par-4 has dual functions by 1) binding to and activating MP when agonist-stimulation is absent; and 2) in the presence of an agonist, facilitating inhibitory phosphorylation of MP by targeting ZIPK. Thus, Par-4 is an amplifier of the *range* of activity of MP.

MATERIALS AND METHODS

Cell Culture

A7r5 rat aorta cells (American Type Culture Collection, Manassas, VA) were cultured in DMEM high glucose (Invitrogen, Carlsbad, CA) with 10% fetal calf serum, 1% glutamine, 50 U/ml penicillin, and 50 μg/ml streptomycin. A7r5 cells were used as a model for smooth muscle that allows the expression of mutant proteins and knockdown by using small interfering RNA (siRNA). A7r5 cells proliferate as myoblasts and, after reaching the stationary phase, differentiate into a phenotype that resembles adult smooth muscle cells (Kimes and Brandt, 1976; Firulli *et al*., 1998). The cells express many smooth muscle specific marker proteins, including smooth muscle α actin, smooth muscle myosin, smooth muscle tropomyosin isoforms, h1 calponin, and SM22 α (Gimona *et al*., 2003). To ensure differentiation of the cells to the smooth muscle-like phenotype, cells were grown to confluence and serum starved for 24 h before all experiments.

In Situ Proximity Ligation Assay (PLA)

For PLA using the Duolink in situ PLA kit (Olink, Uppsala, Sweden), coverslips were stained with the primary antibodies, washed, and further processed essentially according to the manufacturer's instructions. In brief, the coverslips were incubated with the secondary oligonucleotide-linked antibodies provided in the kit. The oligonucleotides bound to the antibodies were hybridized, ligated, amplified, and detected using a fluorescent probe. Dots were detected and counted using NIS Elements AR 2.30 software (Nikon, Melville, NY). Images were processed with Photoshop CS3 software (Adobe Systems, Mountain View, CA).

DNA Constructs

Cloning of the green fluorescent protein (GFP)-tagged and the Strep-tagged Par-4 cDNAs; the GFP-tagged ZIPK cDNA; and cloning of the constructs encoding the C-terminal regions of MYPT1, E2CCLZ (amino acids [aa] 892-1030), CC (aa 924-990), and LZ (aa 992-1030) has been described previously (Kögel *et al*., 1998; Vetterkind *et al*., 2005a,b; Lee *et al*., 2007). For the leucine zipper mutant Par-4 L3A, leucines 295, 316, and 330 were replaced by alanines, as described previously (Boosen *et al*., 2005). The phosphorylation site mutant Par-4 T155A, in which threonine-155 is replaced by an alanine, was generated by site-directed mutagenesis by using the primers 5′-AAG CGC CGC TCC GCT GGC GTG GTC AAC-3′ and 5′-GTT GAC CAC GCC AGC GGA GCG GCG CTT-3′.

Reagents and Antibodies

LPA was purchased from Cayman Chemical (Ann Arbor, MI). Okadaic acid and calyculin A were purchased from Calbiochem (Gibbstown, NJ). Pharmalytes for isoelectric focusing were purchased from GE Healthcare (Little Chalfont, Buckinghamshire, United Kingdom). General laboratory reagents were of analytical grade or better and were purchased from Sigma-Aldrich (St. Louis, MO) and Bio-Rad Laboratories (Hercules, CA). The following primary antibodies were used: rabbit polyclonal anti-PP1cδ antibody (1:250; Millipore, Billerica, MA), rabbit polyclonal anti-M130 antibody (1:1000; Covance Research Products, Princeton, NJ), rabbit polyclonal anti-pT696-MYPT1-antibody (1:500; Millipore), rabbit polyclonal anti-pSer19-LC20 antibody (1:500; Cell Signaling Technology, Danvers, MA), mouse monoclonal anti-LC20 antibody (1:3000; Sigma-Aldrich), mouse monoclonal anti-tubulin α antibody (Sigma-Aldrich), mouse monoclonal anti-GFP antibody (Clontech, Mountain View, CA), and mouse monoclonal anti-Par-4 antibody (1:500; Santa Cruz Biotechnology, Santa Cruz, CA). For immunofluorescence experiments, goat anti-rabbit and goat anti-mouse Alexa Fluor 488 and Alexa Fluor 568 (1:1000; Invitrogen) were used as secondary antibodies. Goat Oregon Green 488- or Alexa Fluor 568-labeled anti-rabbit or anti-mouse immunoglobulin Gs were used as secondary antibodies in Western blot experiments (1:1000; LI-COR Biosciences, Lincoln, NE).

Transfection

Transient transfection using the jetPEI transfection reagent (PolyPlus, New York, NY) was carried out according to the manufacturer's protocol. For Par-4 knockdown experiments, the following cyanine (Cy)3-labeled siRNA oligonucleotides (Dharmacon RNA Technologies, Lafayette, CO) were used: 5′-GAUGCUAUCACACAGCAGA-UU-3′ (antisense) and 3′-UU-CUACGAUAGUGUGUCGUCU-Cy3-5′ (sense) directed against rat Par-4 and 5′-GAUGCAAUUACACAACAGA-UU-3′ (antisense) and 3′-UU-CUACGUUAAUGUGUUGUCU-Cy3-5′ (sense) as mismatch control (directed against human Par-4; Kawai *et al*., 2003). Transfection with 40 nmol/l prehybridized siRNA molecules was performed with Lipofectamine 2000 (Invitrogen) according to the manufacturer's instructions. Cells were processed for experiments 5 d after siRNA transfection.

Immunofluorescence Imaging

Cells were fixed and stained as described previously (Vetterkind *et al*., 2005b). Transfected cells were fixed 48 h after transfection. For some experiments, cells were prepermeabilized with 0.25% Triton X-100 in cytoskeleton stabilization buffer [50 mmol/l NaCl, 3 mmol/l $MgCl_2$, 30 mmol/l sucrose, and 10 mmol/l piperazine-*N*,*N*′-bis(2-ethanesulfonic acid), pH 6.8] for 3 min at 37°C before fixation. Nuclei were stained with 4,6-diamidino-2-phenylindole (Sigma-Aldrich), filamentous actin was stained with Alexa Fluor 568 and Alexa Fluor 488 phalloidin (1:3000; Invitrogen). Cells were examined with an Eclipse TE2000-E fluorescence microscope (Nikon) equipped with a charge-coupled device camera and using filters optimized for double-label experiments.

Immunoprecipitation, Pull-Down Experiments, and Western Blotting

For immunoprecipitation experiments, A7r5 cells were lysed in isotonic lysis buffer (50 mmol/l NaCl, 3 mmol/l $MgCl_2$, 1 mmol/l dithiothreitol, and 0.5% Nonidet-P40 in a 10 mmol/l sodium phosphate buffer, pH 8.0). To prevent protein degradation, lysis buffer was supplemented with a protease inhibitor cocktail (Roche Diagnostics, Indianapolis, IN), and lysates were kept on ice or at 4°C at all times. Lysates were cleared by centrifugation, precleared with empty beads, and subjected to immunoprecipitation with the mouse monoclonal anti-Par-4 antibody (Santa Cruz Biotechnology), the rabbit polyclonal anti-PP1cδ antibody (Millipore) or the rabbit polyclonal anti-GFP antibody (Clontech) at 4°C overnight. The antigen–antibody complexes were adsorbed to protein G-Dynabeads (Invitrogen) and washed three times with lysis buffer. For pull down experiments, purified Par-4 (1 μg) was incubated with an Intein-tagged MYPT1 fragment (aa 850-1030) (Lee *et al*., 2007) immobilized on chitin beads (70 μl). Beads were washed three times with 200 μl of lysis buffer followed by one wash step with kinase buffer (50 mmol/l Tris, 100 mmol/l NaCl, 5 mmol/l $MnCl_2$, and 1 mmol/l dithiothreitol, pH 7.5). A sample of the beads (10 μl) was taken for analysis of Par-4 binding. The remaining beads were split into two samples of 30 μl each. Active ZIPK (0.25 μg; Cell Signaling Technology) was added, and samples were incubated either with or without 50 μM ATP at 37°C for 30 min, followed by three washes with lysis buffer. Samples were taken from all washing steps. Proteins in the samples were separated on 10% SDS polyacrylamide gels according to standard procedures. For Western blot analysis, proteins on SDS gels were transferred onto nitrocellulose membranes (Whatman, Florham Park, NJ). Bound proteins were detected with specific primary antibodies and appropriate secondary antibodies. Bands were visualized on an Odyssey infrared imaging system (LI-COR Biosciences). Densitometry analysis was performed with the Odyssey 2.1 software. Ponceau staining was used to verify equal protein loading and transfer.

Two-dimensional (2-D) Gel Electrophoresis and Glycerol-Urea Gel Electrophoresis

Two-dimensional gel electrophoresis was performed as described previously (Kim *et al*., 2008) by using 0.4% Pharmalytes pH 3–10 and 1.6% Pharmalytes pH 4–6.5 (GE Healthcare). After isoelectric focusing at 400 V for 16 h, tube gels were transferred to 10% SDS polyacrylamide gels. LC20 phosphorylation was measured as an indicator for contractile potential. Glycerol-urea gel electrophoresis was used to separate nonphosphorylated, monophosphorylated, and diphosphorylated light chains as described previously (Kim *et al*., 2000). LC20 phosphorylation (in moles of phosphate per moles of LC20) was calculated from densitometric analyses as follows: [area (monophosphorylated) + 2× area (diphosphorylated)]/[area (unphosphorylated) + area (monophosphorylated) + area (diphosphorylated)].

Phosphatase Assays

Cell lysates were subjected to immunoprecipitation using the anti-PP1cδ antibody (Millipore). Immunoprecipitates were washed three times in lysis buffer and twice in PP1 assay buffer (20 mmol/l Tris-HCl, pH 7.0, 1% Triton X-100, 0.25 mol/l sucrose, 1 mmol/l $MnCl_2$, and 0.1% β-mercaptoethanol) and then split into two equal aliquots and resuspended in phosphatase assay buffer containing 10 mmol/l para-nitrophenyl phosphate (p-NPP; Sigma-Aldrich) as phosphatase substrate and either 5 nmol/l okadaic acid or 5 nmol/l calyculin A as PP1/PP2A inhibitors. PP1 is inhibited by calyculin A at 5 nmol/l but not okadaic acid at 5 nmol/l. Samples, including blank samples, were incubated at 30°C for 2 h. The reaction was stopped by adding 50 mmol/l EDTA. Production of the hydrolysis product para-nitrophenol was measured at 405 nm with a spectrophotometer (Shimadzu, Columbia, MD). To eliminate the activities of potentially copurified/contaminating phosphatases, the activity in the calyculin A sample was subtracted from the activity in the okadaic acid sample, and the remaining calyculin A-sensitive activity was considered as PP1 activity. Specific activity was determined by relating the PP1 activity to the total protein content of the same sample.

Kinase Assays

ZIPK assay reactions were performed in ZIPK assay buffer (50 mmol/l Tris-HCl, pH 7.5, 100 mmol/l NaCl, 5 mmol/l $MnCl_2$, and 1 mmol/l dithiothreitol) in a total volume of 20 μl containing 0.1 μg (1.27 pmol) of active purified recombinant ZIPK (Cell Signaling Technology) and 5 μg of LC20 peptide (BIOMOL Research Laboratories, Plymouth Meeting, PA) as substrate. Where indicated, purified recombinant Par-4 was added in a molar ratio of 1:1 (1.27 pmol) or 10:1 (12.7 pmol). Reactions were incubated for 30 min at 30°C and stopped by adding 10 mmol/l EGTA (end concentration). Then, 2 μl of each reaction was spotted on a nitrocellulose membrane. Bovine serum albumin and LC20 peptide were spotted as controls (each 0.5 μg in 2 μl of kinase assay buffer). The dot blots were blocked and analyzed with anti-Par-4, anti-ZIPK, and anti-pSer19-LC20 antibodies.

Protein Purification

Strep-tagged wild-type Par-4 was expressed in the *Escherichia coli* strain BL21 (DE3) (Stratagene, La Jolla, CA). Bacteria were transformed with Par-4 expression vectors and grown in DYT medium (1.6% tryptone, 1.0% yeast extract, 0.5% NaCl) at 37°C. Protein expression was induced in late log phase with 1 mmol/l isopropyl β-D-thiogalactoside (Sigma-Aldrich). Bacteria were harvested 3 h after induction and solubilized in solubilization buffer (50 mmol/l Tris, pH 7.5, and 200 mmol/l $MgCl_2$) by ultrasonic disruption. Lysates were cleared from cell debris by centrifugation. Recombinant proteins were purified from the cell lysates using StrepTactin Sepharose (IBA, Göttingen, Germany) essentially according to the manufacturer's instructions. The MYPT1 peptides were purified as described previously (Lee *et al*., 2007).

Surface Plasmon Resonance (SPR) Experiments

All SPR experiments were carried out on a BIAcore 3000 (Biacore, Uppsala, Sweden) at 25°C. Sensor chips and reagents for immobilization [1-ethyl-3-(3-dimethylamino-propyl)carbodiimide, *N*-hydroxysuccinimide, and ethanolamine] were purchased from Biacore. Recombinant Par-4 protein was immobilized onto a CM5 sensor chip using the amine coupling method. Typically, 400-1000 resonance units of peptides were immobilized. Running buffer was HEPES-buffered saline containing 10 mmol/l HEPES and 150 mmol/l NaCl, pH 7.4, with 0.005% surfactant P20. Twofold serial dilutions of the MYPT1 peptides CCLZ (aa 925-1030), E2CCLZ (aa 892-1030), CC (aa 925-991), and LZ (aa 992-1030) starting at 348 to 593 μmol/l were used for the binding analysis. SPR data were analyzed using BIAevaluation 4.1 software (Biacore).

Statistical Analysis and Computer-assisted Sequence Analysis

All values given in the text are mean ± SE. Differences between means were evaluated using a two-tailed Student's *t* test. Significant differences were taken at the $p < 0.05$ level. Sequence alignment was performed using the ClustalW server (Larkin *et al*., 2007), and prediction of coiled coil regions and leucine zipper motifs was performed using the 2ZIP server (Bornberg-Bauer *et al*., 1998).

RESULTS

Par-4 Interacts with MP in Smooth Muscle Cells

In immunofluorescence experiments with the rat aorta cell line A7r5, endogenous Par-4 colocalizes with endogenous PP1cδ and endogenous MYPT1 along the actin cables (Supplemental Figure S1). To find out whether Par-4 interacts with PP1cδ and/or MYPT1 in vivo, coimmunoprecipitation experiments using a monoclonal anti-Par-4 antibody were performed. As shown in Figure 1A, endogenous PP1cδ and MYPT1 were coprecipitated with endogenous Par-4 but not in control experiments. Moreover, after immunoprecipitation of endogenous PP1cδ with an anti-PP1cδ antibody, both MYPT1 and Par-4 bands could be detected. Because Par-4 does not contain a PP1 binding motif but harbors a C-terminal leucine zipper motif, we speculated that binding of Par-4 to MP could be mediated by leucine zipper-leucine zipper interaction between Par-4 and MYPT1. To test this hypothesis, we performed coimmunoprecipitation experiments with transfected A7r5 cells overexpressing GFP-tagged wild-type Par-4 or a Par-4 mutant in which three leucines of the leucine zipper have been replaced by alanines (L3A) (Boosen *et al*., 2005). Supplemental Figure S2 shows the sequence of the Par-4 leucine zipper and the position of the mutated leucines in L3A. In immunoprecipitation experiments with an anti-GFP antibody, endogenous MYPT1 coimmunoprecipitated with wild-type Par-4-GFP, whereas the amount of MYPT1 that was coimmunoprecipitated with the Par-4 leucine zipper mutant L3A-GFP was significantly reduced, indicating that the leucine zipper of Par-4 mediates binding to MYPT1 (Figure 1B). Coimmunoprecipitation of PP1cδ and the Par-4 interaction partner ZIPK with L3A-GFP were also reduced. Because the association of Par-4 with the MP complex depends on the presence of the Par-4 leucine zipper, it seems likely that binding to the MP complex is mediated by a leucine zipper-leucine zipper interaction between Par-4 and MYPT1.

Endogenous interaction was confirmed by the in situ PLA, an immunofluorescence-based method that generates a quantifiable signal indicative of proximity (30–50 nm) between two antigens (Fredriksson *et al*., 2002; Greenberg *et al*., 2008; Söderberg *et al*., 2008; Mellberg *et al*., 2009). Control experiments showed that staining with each antibody alone (instead of antibody pairs) resulted in virtually no signal in any case (data not shown). As is shown in Figure 1C, the Par-4 and MYPT1 antibody pair produced a significantly higher PLA signal than a negative control antibody pair (MYPT1 and tubulin), and the Par-4 and MYPT1 PLA signal was of similar magnitude to that of a positive control antibody pair (LC20 and pSer19-LC20), indicating that Par-4 and MYPT1 are in proximity to each other in the cell, probably in the same protein complex. Furthermore, in cells transfected with either wild-type Par-4-GFP or the leucine zipper mutant L3A-GFP, the number of dots was significantly higher in cells transfected with Par-4 than in cells transfected with the leucine zipper mutant (Figure 1C), confirming a role for the Par-4 leucine zipper in binding to MYPT1.

Direct binding of Par-4 and MYPT1 was assayed by SPR experiments. For this purpose, purified recombinant wild type Par-4 was immobilized on a CM 5 sensor chip and tested for binding of specific purified MYPT1 peptides E2CCLZ (aa 891-1030), CCLZ (aa 924-1030), CC (aa 924-990), and LZ (aa 991-1030) (Lee *et al*., 2007). The data in Figure 1D show that Par-4 binds to LZ but not CC; similar results as those for LZ were obtained for E2CCLZ and CCLZ (data not shown), indicating that Par-4 binds to LZ and to peptides that contain LZ. Thus, the leucine-zipper of Par-4 binds the leucine zipper domain of MYPT1. An apparent dissociation constant (k_d) of 84 μmol/l, a likely overestimate because it does not take into account homodimerization of Par-4, was determined for binding of Par-4 and CCLZ. However, because purified Par-4 was not compatible with the buffer requirements for SPR flow channel, we were not able to calculate the k_d value for Par-4 dimerization and therefore cannot provide an accurate k_d value for interaction of Par-4 and MYPT1.

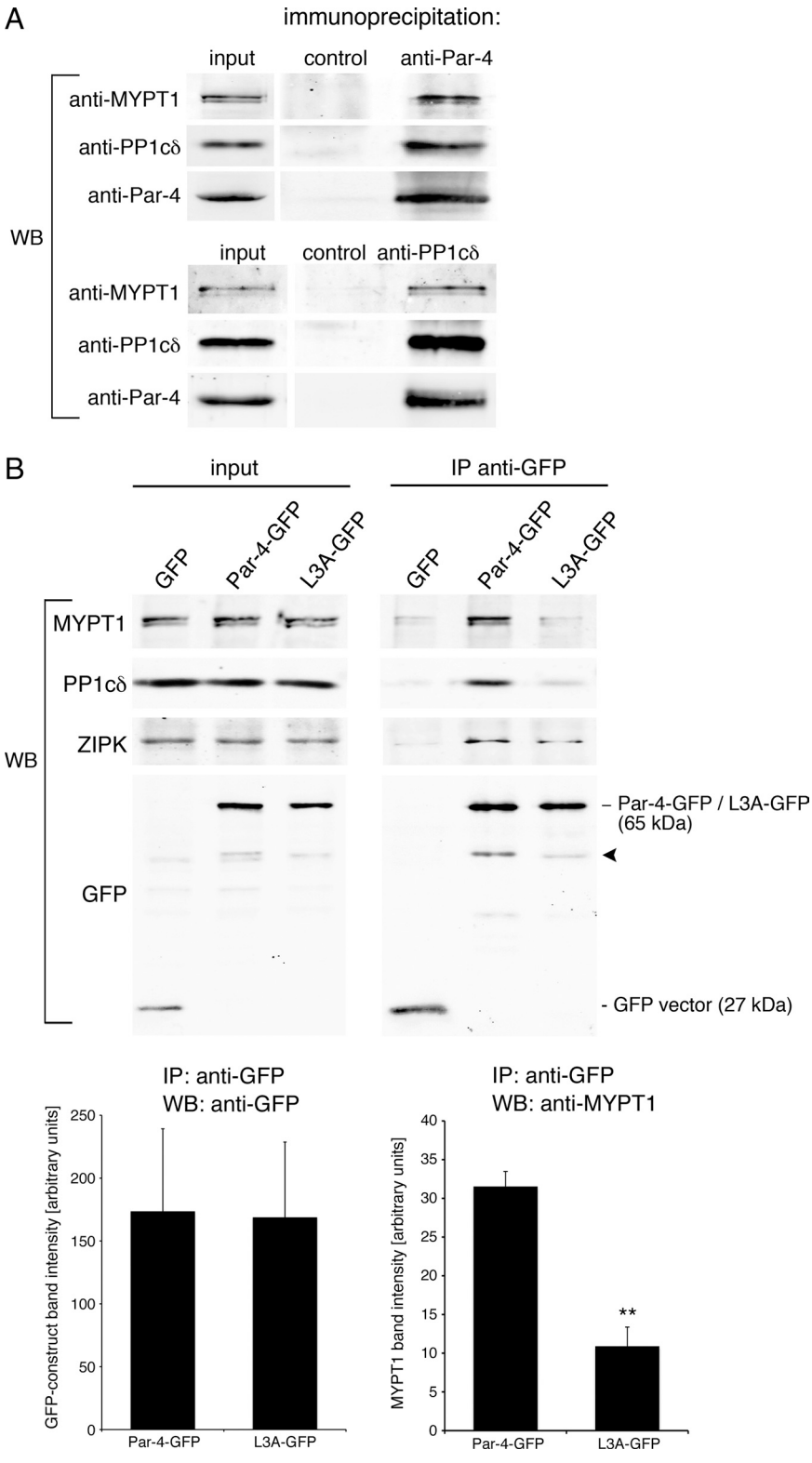

Figure 1. Interaction of Par-4 with the subunits of MP. (A) Endogenous interactions. A7r5 cell lysates were subjected to immunoprecipitation with an anti-Par-4 antibody or an anti-PP1cδ antibody as indicated. Endogenous PP1cδ, MYPT1 and Par-4 were detected by Western blot analysis. Protein G-beads alone served as control. (B) Identification of binding domain. A7r5 lysates from cells transfected with either GFP, wild-type Par-4-GFP, or L3A-GFP were subjected to immunoprecipitation with an anti-GFP antibody. Immunoprecipitated GFP-constructs and coimmunoprecipitated endogenous MYPT1, ZIPK and PP1cδ were detected with specific antibodies. Arrowhead, nonspecific bands. The graphs shows mean densitometric values for immunoprecipitated Par-4-GFP and L3A-GFP (efficiency of IP, left) and coimmunoprecipitated MYPT1 (right) from three independent experiments. (C) Conformation of interaction by proximity ligation assay. A7r5 cells (either untransfected or transfected with Par-4-GFP or L3A-GFP as indicated) were fixed and incubated with MYPT1 and tubulin antibodies as negative control, LC20 and pSer19-LC20 antibodies as positive controls, and MYPT1 and Par-4 antibodies. The number of signal dots, as a measure for proximity of an antigen pair (see immunofluorescence panel, inverted for better visualization), was analyzed based on 20 cells per antigen pair and in four independent experiments. Representative microscopic images are shown for the tests with untransfected cells. Bar, 20 μm. (D) Direct interaction is shown by surface plasmon resonance. Top, Domain map of full-length MYPT1 showing the position of ankyrin repeats (green), basic regions (magenta) containing the two inhibitory phosphorylation sites T696 and T853, coiled coil regions (CC; blue), and the leucine zipper motif (LZ; yellow). MYPT1 peptides LZ and CC were injected onto a surface plasmon resonance chip presenting immobilized full length Par-4. The sensorgrams show the response difference from a reference channel without immobilized protein. Series of twofold dilutions of the analyte (red curve, highest concentration) were analyzed (*$p < 0.05$, **$p < 0.01$, and ***$p < 0.001$).

Par-4 Bound to MP Is Primarily Unphosphorylated

Par-4 is a phosphoprotein that is known to be regulated by upstream kinases such as ZIPK, PKA, and PKB/Akt (Page *et al*., 1999; Kawai *et al*., 2003; Goswami *et al*., 2005; Gurumurthy *et al*., 2005). To find out whether Par-4 phosphorylation is required for Par-4 binding to MP, we analyzed the phosphorylation state of Par-4 by 2-D gel electrophoresis before (Figure 2A, black bars) and after (Figure 2A, white bars) coimmunoprecipitation with PP1cδ. That the anti-PP1cδ antibody is able to coimmunoprecipitate MYPT1 is shown in Figure 1A. Par-4 spots were detected with a specific anti-Par-4 antibody. In pilot studies, phosphorylated and un-

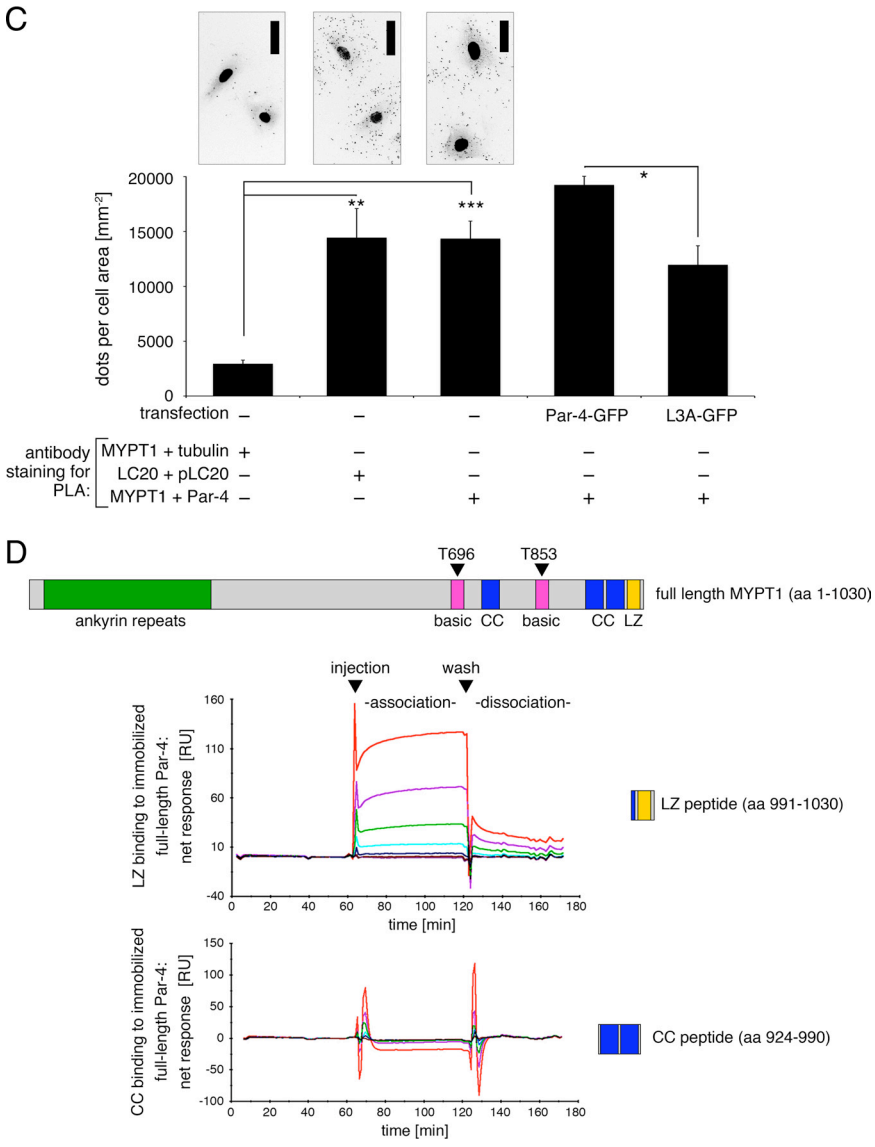

Figure 1. *Continued.*

phosphorylated Par-4 spots were identified by analyzing samples that were subjected to phosphatase and phosphatase inhibitor treatments (Supplemental Figure S3A). As shown in Figure 2A, densitometric analysis of 2-D gels indicates that in unstimulated cells, ~30% of Par-4 is phosphorylated. After stimulation with LPA to induce Rho/Rho kinase (ROCK) and ZIPK activation, Par-4 phosphorylation levels were significantly increased to 45%. However, after immunoprecipitation of MP with an anti-PP1cδ antibody, the phosphorylation levels of coprecipitated Par-4 (white bars in Figure 2A) were indistinguishable between LPA stimulated and unstimulated cell extracts (26 and 29%, respectively). Control experiments showed that the phosphorylation state of Par-4 was preserved throughout the experiment (Supplemental Figure S3B). These results suggest that the majority of Par-4 bound to MP is unphosphorylated and that Par-4 phosphorylation is not required for binding to MP. To test whether phosphorylation of Par-4 might weaken the interaction with MYPT1, we have performed in vitro experiments with purified Par-4, an immobilized purified C-terminal MYPT1 fragment, and purified active ZIPK. We show in Figure 2B that Par-4 binds to the immobilized MYPT1 fragment (Figure 2B, input) and that it is released from the beads into the wash buffer upon addition of active ZIPK in the presence, but not in the absence, of ATP (Figure 2B). In addition, we show in Figure 2C that MYPT1 is coprecipitated with both wild type Par-4 and a phosphorylation site mutant (T155A) in untreated cells, whereas after LPA stimulation, coimmunoprecipitation of MYPT1 could only be detected for the phosphorylation site mutant. These results demonstrate that Par-4 binds to MP preferentially when it is unphosphorylated, whereas Par-4 phosphorylation, because it occurs after stimulation of Rho/ROCK and ZIPK by LPA, leads to its detachment from the MP complex.

Par-4 Supports PP1 Activity

To find out whether interaction with Par-4 affects MP activity, we assayed the activity of immunoprecipitated PP1 holoenzymes after overexpression of Par-4 or the leucine zipper mutant of Par-4 L3A. Proteins were overexpressed threefold to fivefold over endogenous Par-4. Interestingly, phosphatase activity was increased approximately threefold in Par-4–transfected cells compared with untransfected or GFP-transfected cells (Figure 3A). In L3A-expressing cells,

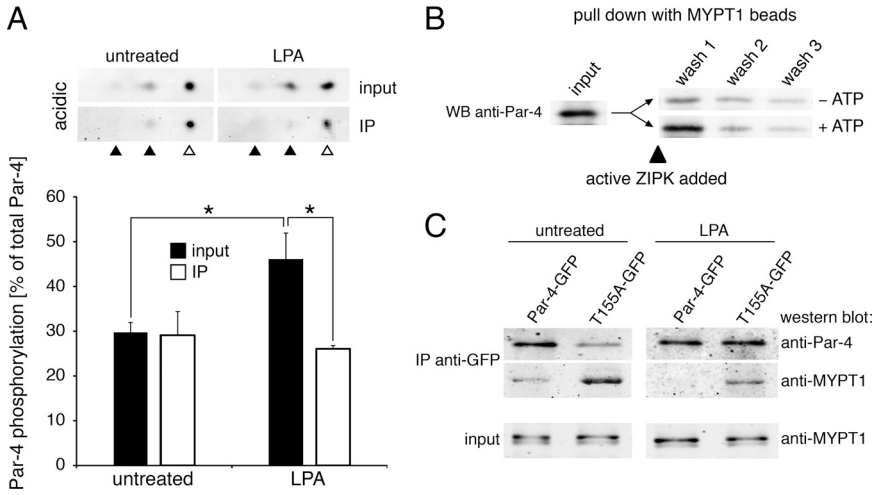

Figure 2. Par-4 phosphorylation reduces binding to MP. (A) A7r5 cells were treated with 10 μmol/l LPA for 15 min, or untreated. One tenth of cell lysate was saved and prepared for isoelectric focusing (=input sample, black bars), and the remainder subjected to immunoprecipitation with an anti-PP1cδ antibody. Immunoprecipitates were subjected to isoelectric focusing (=IP, white bars) followed by regular SDS-polyacrylamide gel electrophoresis and Western blotting (shown on top). Black arrowheads, phosphorylated Par-4; open arrowheads, unphosphorylated Par-4. The graph shows averages of three to four independent experiments (*$p < 0.05$). (B) In vitro experiment showing release of Par-4 from MYPT1 beads after incubation with active ZIPK. Purified Par-4 was incubated with an immobilized purified MYPT1 fragment (aa 850-1030). After washing, a sample of the beads was removed for analysis of Par-4 binding (input). The remaining beads were split into two reactions. Active ZIPK was added to both reactions; however, ATP was added only to one reaction. After incubation at 37°C for 30 min, the beads were washed three times. Samples of input and washing steps were analyzed by Western blotting with an anti-Par-4 antibody (three independent experiments were performed). (C) A7r5 cells were transfected with either wild-type Par-4-GFP or the phosphorylation site mutant T155A-GFP and subjected to immunoprecipitation with an anti-GFP antibody. MYPT1 was coprecipitated with GFP-tagged wild-type Par-4 and T155A in unstimulated cells; however, after stimulation with LPA, MYPT1 was only coimmunoprecipitated in the cells overexpressing the phosphorylation site mutant T155A. One representative out of three independent experiments is shown.

PP1 activity was significantly lower than in Par-4–transfected cells and remained at the level of background PP1 activity (Figure 3A). To further test the hypothesis that Par-4 increases MP activity, we applied a knockdown approach. Endogenous Par-4 protein expression was down-regulated in the rat smooth muscle cell line A7r5 by using siRNA directed against rat Par-4. As a mismatch control, we used siRNA directed against human Par-4 (which differs in sequence by three nucleotides). In Par-4 siRNA-transfected cells, the Par-4 expression was significantly reduced to an average of 37% of that in the mismatch transfected cells, whereas expression of MYPT1, ZIPK, and PP1cδ was unaffected by the knockdown (Supplemental Figures S4, A and B). In the same experiments, PP1 activity was significantly reduced in the Par-4 siRNA-treated cells compared with the mismatch treated cells (0.015 ± 0.0029 vs. 0.041 ± 0.0057 U; Figure 3A).

Par-4 Leads to Reduced LC20 Phosphorylation Levels

In combination with various regulatory subunits, PP1cδ is active against a wide array of different substrates (for review, see Ceulemans and Bollen, 2004). To specifically analyze the effect of Par-4 on PP1cδ as part of the MP holoenzyme, we monitored LC20 phosphorylation after overexpression of Par-4. For this purpose, we applied the proximity ligation assay using a mouse monoclonal anti-LC20 antibody and a rabbit polyclonal pSer19-LC20 antibody as primary antibodies, so that a signal is generated when LC20 is phosphorylated at serine 19, but not when it is unphosphorylated. This cell-based assay, in contrast to a traditional gel-based assay, has the advantage of allowing selected analysis of the subpopulation of transfected cells. Consistent with the activation of PP1 described above, overexpression of Par-4 led to reduced LC20 phosphorylation levels (Figure 3B). In contrast, expression of L3A, which is impaired in binding to MYPT1, had no effect on LC20 phosphorylation, indicating that Par-4 activates MP via binding to MYPT1 (Figure 3B). Overexpression of wild-type Par-4 with ZIPK had no effect over that of ZIPK alone. However, a Par-4 phosphorylation site mutant, T155A, which would prevent the displacement of Par-4 from MYPT1 and lead to an increased MP activity, decreased the phosphorylation level of LC20 compared with ZIPK alone (Figure 3B and model in Figure 4C). Competitive peptide blocking experiments were performed to test the specificity of the pSer19-LC20-antibody in the context of the proximity ligation assay. As shown in Figure 3C (inverted immunofluorescence images and graph), preincubation of the anti-pSer19-LC20 antibody with an unphosphorylated LC20 peptide containing the Ser19 phosphorylation site did not affect the number of signal dots. However, preincubation of the phospho-antibody with the same peptide after it had been phosphorylated by ZIPK, led to a significantly reduced signal in the PLA assay. The proximity ligation assay with the anti-LC20/anti-pSer19-LC20 antibody pair was also sensitive enough to detect changes in LC20 phosphorylation levels in A7r5 cells after treatment with the MLCK inhibitor ML-9 or with the PP1 and PP2B inhibitor calyculin A (graph in Figure 3C). Specificity of the pSer19-LC20 antibody is further shown in Figure 3C in a glycerol-urea gel analysis of A7r5 lysate.

Par-4 Has a Dual Function as an Activator and Inhibitor of MP

In a previous publication, we have reported that knockdown of Par-4 leads to a reduced response of smooth muscle strips to agonist stimulation, indicating a role for Par-4 in inhibition of MP (Vetterkind and Morgan, 2009). Here, our findings show that Par-4 activates MP in resting cultured smooth muscle cells. To test whether Par-4 might have a dual function in the regulation of MP, we have performed siRNA knockdown of Par-4 in A7r5 cells, followed by Western blot to analyze MYPT1 phosphorylation at threonine 696, the phosphorylation site preferred by ZIPK (MacDonald *et al.*, 2001; Borman *et al.*, 2002). In smooth muscle, MYPT1 phosphorylation at threonine 696 can be detected upon contractile stimulation and seems to be involved in calcium sensitization and steady-state contraction rather than initial contraction (Shin *et al.*, 2002; Mizuno *et al.*, 2008; Ding *et al.*, 2009; Khromov *et al.*, 2009). LC20 phosphorylation was analyzed by glycerol-urea gel electrophoresis. Cells were stimulated with LPA, or left untreated, before quick freezing in

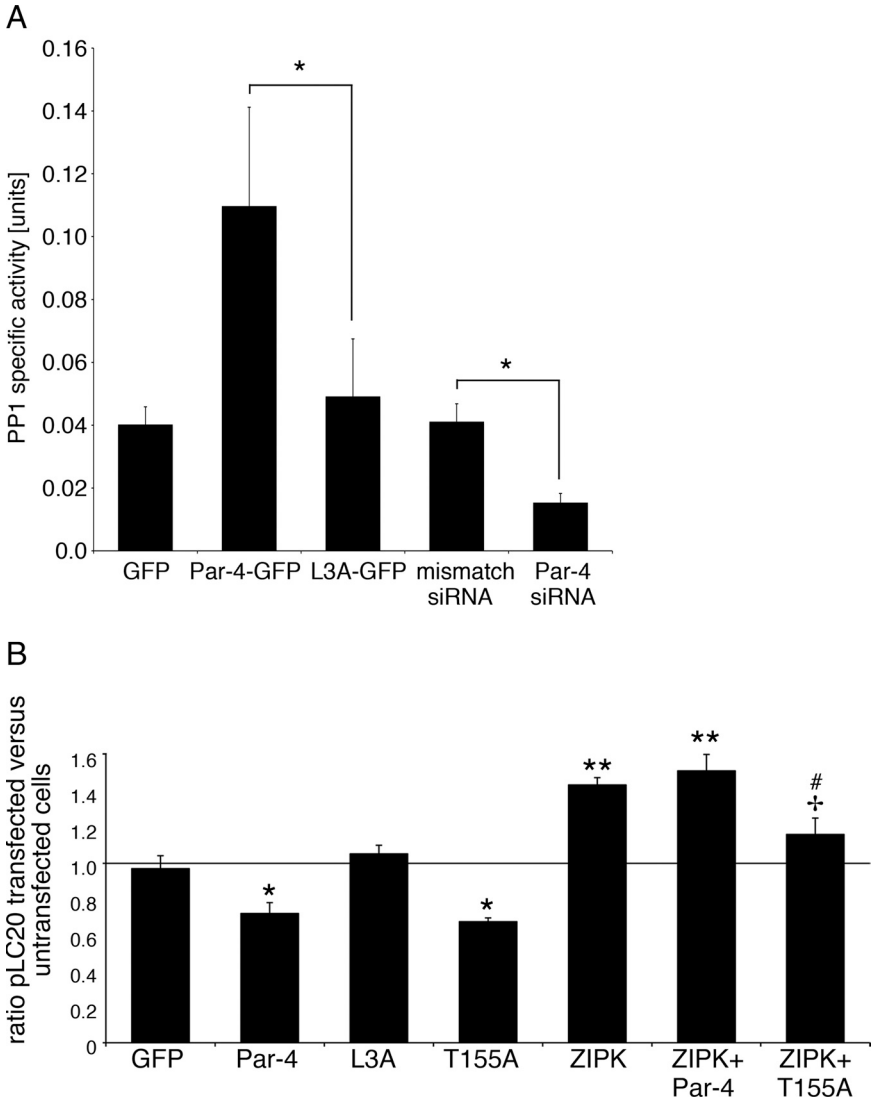

Figure 3. Par-4 regulates MP activity. (A) Par-4 activates PP1cδ. A7r5 cells transfected with GFP, Par-4-GFP, L3A-GFP, mismatch siRNA, or Par-4 siRNA were subjected to immunoprecipitation with an anti-PP1cδ antibody. Immunoprecipitates were subjected to a phosphatase assay using p-NPP as substrate (*p = 0.029 and 0.018, paired two-tailed *t* test). (B) Dual function of Par-4 for LC20 phosphorylation. A7r5 cells were transfected with different Par-4 constructs and/or ZIPK as indicated. Cells were fixed, incubated with anti-LC20 and pSer19-LC20 antibodies and subjected to the proximity ligation assay. The graph shows averages from five to six independent experiments. The ratio of dots per area in transfected versus nontransfected cells is shown for each transfected DNA or DNA combination (*$p < 0.05$ and **$p < 0.01$, compared with GFP control; #$p < 0.05$ compared with ZIPK; +$p < 0.05$ compared with ZIPK+Par-4, unpaired *t* test). (C) Controls for PLA-based LC20 phosphorylation assays using the anti-LC20 and pSer19-LC20 antibody pair. For competitive blocking, the pSer19-LC20 antibody was preincubated with a nonphosphorylated or phosphorylated LC20 peptide as indicated before PLA staining. To assess the sensitivity of the PLA method, endogenous LC20 phosphorylation levels were changed by treating A7r5 cells with the MLCK inhibitor ML-9 or the PP1 and PP2A inhibitor Calyculin A as indicated. The graph shows the statistical analyses with each bar representing three independent experiments with 20 cells each (***$p < 0.001$). Representative immunofluorescence images are shown for competitive blocking of PLA signal. The Western blot shows specificity of the anti-pSer19-LC20 antibody toward phosphorylated LC20 in A7r5 cell lysates prepared in urea sample buffer and separated by glycerol/urea gel. (D) Changes in MYPT1 and LC20 phosphorylation after knockdown of Par-4. A7r5 cells were transfected with siRNA directed against rat Par-4. As mismatch control, siRNA directed against human Par-4 was used. Cells were either left untreated, or stimulated with LPA, followed by quick-freezing in TCA/acetone. Cell lysates were either analyzed by Western blot with the anti-MYPT1 antibody and the phospho-specific anti-pT696-MYPT1 antibody (top and middle panel, each representing one out of three independent experiments) or by glycerol-urea gel electrophoresis followed by Western blot analysis using an anti-LC20 antibody (bottom). Note that after Par-4 knockdown, LC20 phosphorylation is increased in unstimulated cells, but decreased in LPA-stimulated cells. The graph shows the statistical analysis of LC20 phosphorylation from six independent experiments (*$p < 0.05$, paired two-tailed *t* test). (E) Par-4 does not interfere with ZIPK mediated LC20 phosphorylation directly. Kinase assay with purified recombinant ZIPK and an LC20 peptide as substrate. Reactions were incubated in the presence or absence of purified recombinant Par-4 as indicated. Samples were spotted on nitrocellulose membranes and analyzed for phosphorylation of the LC20 peptide with the phospho-specific LC20 antibody.

trichloroacetic acid/acetone. As shown in Figure 3D, in Par-4 knockdown cells MYPT1 inhibitory phosphorylation at threonine 696 is elevated in unstimulated cells but reduced in LPA-treated cells, compared with mismatch siRNA-transfected cells. Consistently, LC20 phosphorylation is increased after Par-4 knockdown in untreated cells, but significantly reduced in LPA stimulated cells (see graph in Figure 3D for statistical analysis). These results are in agreement with our previous findings that in vascular smooth muscle, Par-4 acts as an inhibitor of MP during agonist stimulation. At the same time, these findings are consistent with the other findings presented here, identifying Par-4 as an activator of MP in unstimulated cells. Furthermore, when the data that were generated with differentiated smooth muscle in the previously published work (Vetterkind and Morgan, 2009) were analyzed retrospectively for basal tone, it was revealed that antisense knockdown of Par-4 not only reduces PGF-2α-induced contraction (Vetterkind and Morgan, 2009) but also increases basal tone (Supplemental Figure S4C), consistent with the finding that Par-4 supports MP activity in unstimulated cells. These results indicate that Par-4 has dual functions: 1) as an activator of MP in the absence of agonists and 2) as an inhibitor of MP in the presence of an agonist. Because ZIPK can phosphorylate LC20 directly (Kögel *et al*., 1998; Murata-Hori *et al*., 1999), we tested for direct regulation of ZIPK activity by Par-4 in a kinase assay using an LC20 peptide as substrate. As shown in Figure 3E, phosphorylation of the LC20 peptide

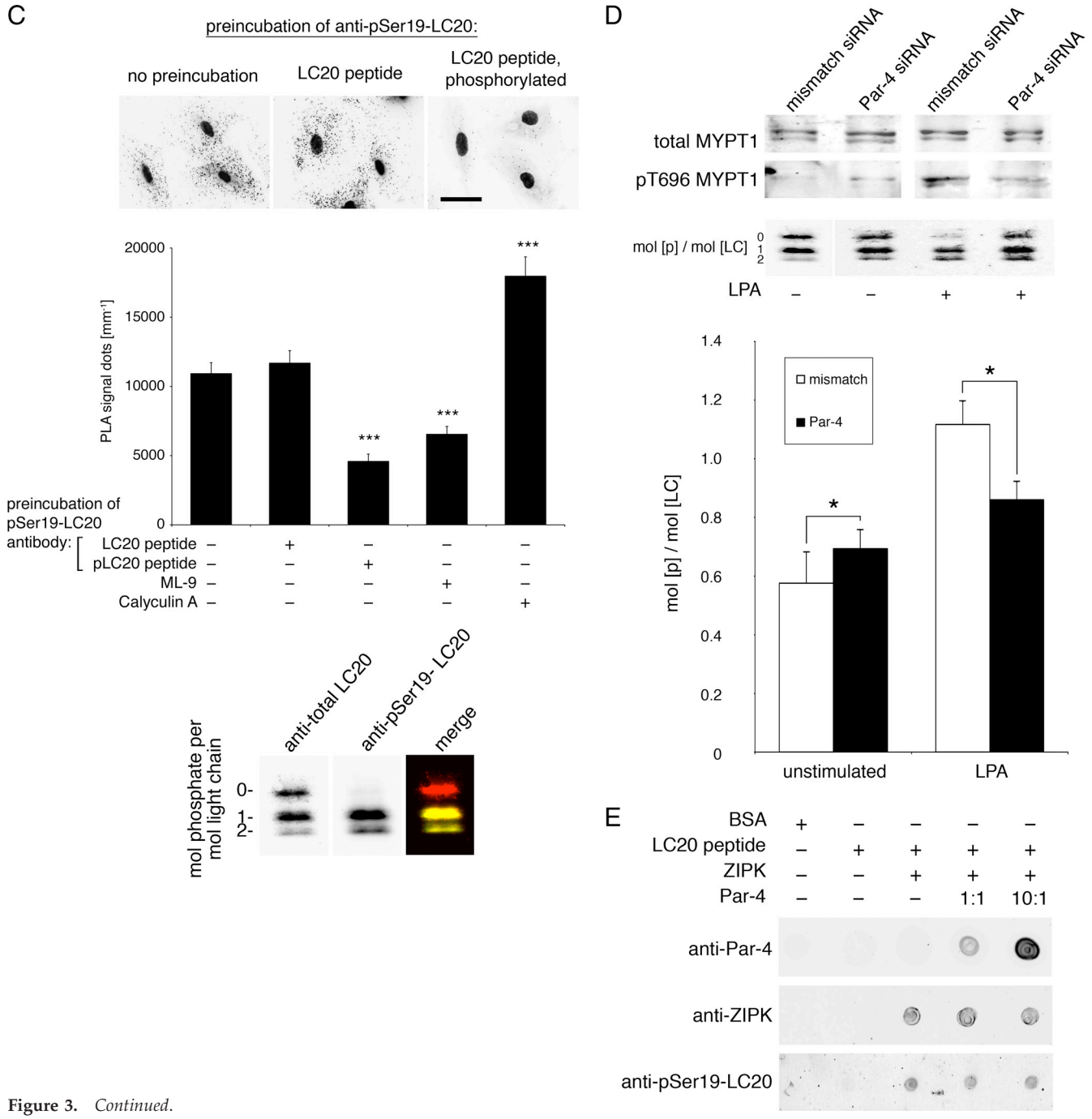

Figure 3. *Continued.*

by ZIPK was not affected by the presence of Par-4, thus ruling out direct regulation of ZIPK by Par-4.

DISCUSSION

The major finding of this work is the identification of Par-4 as an activator of MP. Many inhibitors of MP are known, including CPI-17 (Eto *et al.*, 1995) as well as several kinases that target MYPT1: Rho/Rho kinase (Kimura *et al.*, 1996; Feng *et al.*, 1999), ZIPK (Figure 4A; MacDonald *et al.*, 2001; Endo *et al.*, 2004), and ILK (Kiss *et al.*, 2002; Muranyi *et al.*, 2002). In contrast, the NO pathway is the single most important signaling cascade demonstrated thus far to activate MP in smooth muscle cells (Surks *et al.*, 1999). The effects of NO are primarily mediated by PKG (Nakamura *et al.*, 1999; Wooldridge *et al.*, 2004). Here, we add another activator of MP, Par-4, to the network regulating the phosphorylation state of LC20 and hence the level of contractile potential.

Based on our results, we suggest the following model to complement the current view of MYPT1 inhibitory phosphorylation (shown here for ZIPK, as an example; Figure 4A). Par-4 acts as a molecular "padlock" to maintain MP in an activated state (Figure 4B). Par-4 knockdown decreases basal MP activity (Figure 3, A and D; also see model in Figure 4A). Par-4, in its unphosphorylated state, binds to MP via interaction with MYPT1. Our previously published work has shown that Par-4

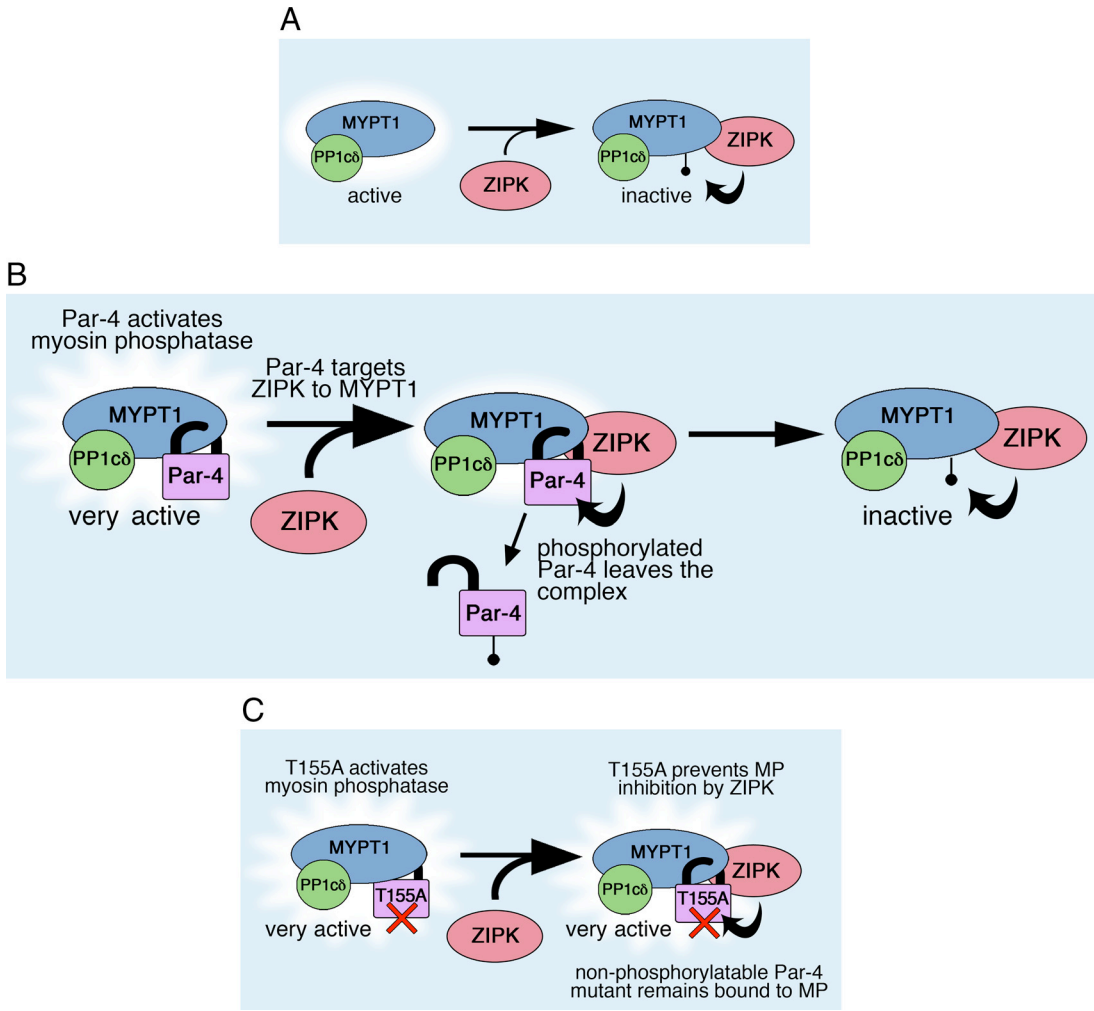

Figure 4. Model: Par-4 as a molecular padlock for MP. (A) MP is active until it is phosphorylated at the C-terminal inhibitory phosphorylation site T696 by ZIPK. (B) Binding of Par-4 enhances phosphatase activity. Par-4 targets ZIPK to the MP complex (Vetterkind and Morgan, 2009), but at the same time, like a padlock, blocks access to the inhibitory phosphorylation site. After phosphorylation ("unlocking") of Par-4 by ZIPK ("key"), Par-4 leaves the MP complex and the inhibitory phosphorylation site inaccessible for inhibitory phosphorylation. (C) A Par-4 phosphorylation site mutant, T155A, interferes with ZIPK-mediated MP inhibition. T155A binds to and activates MP; however, as it cannot be phosphorylated, it remains bound to MP even in the presence of active ZIPK, and prevents inhibitory phosphorylation of MYPT1 by ZIPK.

targets ZIPK to the MP complex and supports MYPT1 phosphorylation by ZIPK (Vetterkind and Morgan, 2009). Our finding that a nonphosphorylatable T155A Par-4 mutant prevents inhibition of MP by ZIPK (Figure 3B and model in Figure 4C) suggests that binding of Par-4 restricts the access of ZIPK, and possibly other MYPT1 kinases like ROCK and ILK, to the C-terminal inhibitory phosphorylation site(s) on MYPT1 and, in essence "locks" MP in the activated state. Once phosphorylated, Par-4 leaves the MP complex, so that MP is "unlocked" from the activated state and MYPT1 can be phosphorylated (Figure 4B). The observed increase in MP activity by Par-4 overexpression (Figure 3B) may result solely from a prevention of inhibition of MP by basal MYPT1 kinase activities; however, physical stabilization of the MP complex by binding of Par-4 is also possible.

The results presented here used LC20 phosphorylation as an endpoint, but when they are taken together with our past results in smooth muscle tissue (Vetterkind and Morgan, 2009), suggest a mechanism by which Par-4 regulates contractility. Together, these results predict that Par-4 has dual actions in the regulation of vascular tone and thus solve an apparent paradox between the direct activating effect of Par-4 on MP (which would inhibit contractility) and the previously described inhibition of agonist-induced contractility by Par-4 knockdown in smooth muscle tissue (Vetterkind and Morgan, 2009). It is important to note that the previously published data relate to agonist-stimulated smooth muscle, whereas in the present work, we have used unstimulated cultured smooth muscle cells. Thus, as predicted by our model, in the absence of agonist stimulation, the ZIPK pathway is not recruited and Par-4 overexpression has a net activating effect on MP and inhibits contractile activity. Alternatively, agonist stimulation would activate ZIPK (or other pathways) that require Par-4 as a scaffold to be targeted to MP. With Par-4 knockdown, targeting of ZIPK will be reduced (Vetterkind and Morgan, 2009) and the consequent ZIPK-mediated inhibition of MP diminished, explaining a decrease in contractility. Thus, these data indicate that although Par-4 promotes MP activity in unstimulated cells, Par-4 also supports ZIPK-mediated inhibition of MP once ZIPK is activated. Although the data presented here indicate that Par-4 promotes phosphorylation of MYTP1 at threonine 696 after

LPA stimulation, we cannot rule out that the effect of Par-4 on MP activity might be partially mediated by the other C-terminal inhibitory phosphorylation site, threonine 853, because this site, although primarily phosphorylated by ROCK, can be phosphorylated by ZIPK in vitro (Borman *et al*., 2002). Furthermore, because ZIPK and ROCK have similar consensus phosphorylation sites and overlapping substrate spectra, it seems possible that Par-4 could be a downstream target of ROCK as well.

The findings and the model presented here are also relevant for the apoptotic functions of Par-4. Our finding that Par-4 is required for ZIPK-mediated LC20 phosphorylation (Figure 3B) is in agreement with a proapoptotic function for Par-4 that is based on Par-4–mediated targeting of ZIPK to the cytoskeleton and to MP (Page *et al*., 1999; Vetterkind *et al*., 2005b; Vetterkind and Morgan, 2009). The inhibition of MP, in the context of apoptosis, can be regarded as a proapoptotic event, because the resulting LC20 phosphorylation has been causatively linked to apoptosis (Petrache *et al*., 2001; Lai *et al*., 2003).

Similarly, our findings and model are of interest in reference to the fact that some members of the ATP-binding cassette kinase family that require auto/transphosphorylation for activation (Burgering and Coffer, 1995; Andjelkovic *et al*., 1996; Kohn *et al*., 1996; Wooten *et al*., 1996) are regulated by Par-4. Probably the best-studied apoptotic Par-4 function in the cytoplasm is the inhibition of aPKCζ (Diaz-Meco *et al*., 1996; Leroy *et al*., 2005; Wang *et al*., 2005) and PKB/Akt (Joshi *et al*., 2008; Lee *et al*., 2008), two prosurvival kinases. It has been shown that knockdown of Par-4 leads to enhanced Akt phosphorylation levels (Joshi *et al*., 2008). This suggests that in the regulation of aPKCζ and Akt, Par-4 might also act as a molecular padlock to prevent activating phosphorylation of Akt and/or aPKCζ.

In summary, we have shown, for the first time, that Par-4 directly binds to and activates MP. We have also demonstrated that Par-4 is required for agonist-induced, ZIPK-mediated inhibition of MYPT1 and thus is an important amplifier of inputs to MP.

ACKNOWLEDGMENTS

We are grateful for the rat ZIPK (Dlk) cDNA from Karl-Heinz Scheidtmann (University of Bonn, Bonn, Germany). This work was supported by National Institutes of Health grants HL-31704, HL-80003, HL-86655, and AR-49066 and by a postdoctoral fellowship (to S. V.) from the American Heart Association.

REFERENCES

Alessi, D., MacDougall, L. K., Sola, M. M., Ikebe, M., and Cohen, P. (1992). The control of protein phosphatase-1 by targetting subunits. The major myosin phosphatase in avian smooth muscle is a novel form of protein phosphatase-1. Eur. J. Biochem. *210*, 1023–1035.

Andjelkovic, M., Jakubowicz, T., Cron, P., Ming, X. F., Han, J. W., and Hemmings, B. A. (1996). Activation and phosphorylation of a pleckstrin homology domain containing protein kinase (RAC-PK/PKB) promoted by serum and protein phosphatase inhibitors. Proc. Natl. Acad. Sci. USA *93*, 5699–5704.

Boosen, M., Vetterkind, S., Koplin, A., Illenberger, S., and Preuss, U. (2005). Par-4-mediated recruitment of Amida to the actin cytoskeleton leads to the induction of apoptosis. Exp. Cell Res. *311*, 177–191.

Borman, M. A., MacDonald, J. A., Muranyi, A., Hartshorne, D. J., and Haystead, T. A. (2002). Smooth muscle myosin phosphatase-associated kinase induces Ca2+ sensitization via myosin phosphatase inhibition. J. Biol. Chem. *277*, 23441–23446.

Bornberg-Bauer, E., Rivals, E., and Vingron, M. (1998). Computational approaches to identify leucine zippers. Nucleic Acids Res. *26*, 2740–2746.

Burgering, B. M., and Coffer, P. J. (1995). Protein kinase B (c-Akt) in phosphatidylinositol-3-OH kinase signal transduction. Nature *376*, 599–602.

Ceulemans, H., and Bollen, M. (2004). Functional diversity of protein phosphatase-1, a cellular economizer and reset button. Physiol. Rev. *84*, 1–39.

Cheema, S. K., Mishra, S. K., Rangnekar, V. M., Tari, A. M., Kumar, R., and Lopez-Berestein, G. (2003). Par-4 transcriptionally regulates Bcl-2 through a WT1-binding site on the bcl-2 promoter. J. Biol. Chem. *278*, 19995–20005.

Chen, Y. H., Chen, M. X., Alessi, D. R., Campbell, D. G., Shanahan, C., Cohen, P., and Cohen, P. T. (1994). Molecular cloning of cDNA encoding the 110 kDa and 21 kDa regulatory subunits of smooth muscle protein phosphatase 1M. FEBS Lett. *356*, 51–55.

Diaz-Meco, M. T., Municio, M. M., Frutos, S., Sanchez, P., Lozano, J., Sanz, L., and Moscat, J. (1996). The product of par-4, a gene induced during apoptosis, interacts selectively with the atypical isoforms of protein kinase C. Cell *86*, 777–786.

Ding, H. L., Ryder, J. W., Stull, J. T., and Kamm, K. E. (2009). Signaling processes for initiating smooth muscle contraction upon neural stimulation. J. Biol. Chem. *284*, 15541–15548.

Dirksen, W. P., Vladic, F., and Fisher, S. A. (2000). A myosin phosphatase targeting subunit isoform transition defines a smooth muscle developmental phenotypic switch. Am. J. Physiol. Cell Physiol. *278*, C589–C600.

Endo, A., Surks, H. K., Mochizuki, S., Mochizuki, N., and Mendelsohn, M. E. (2004). Identification and characterization of zipper-interacting protein kinase as the unique vascular smooth muscle myosin phosphatase-associated kinase. J. Biol. Chem. *279*, 42055–42061.

Eto, M., Ohmori, T., Suzuki, M., Furuya, K., and Morita, F. (1995). A novel protein phosphatase-1 inhibitory protein potentiated by protein kinase C. Isolation from porcine aorta media and characterization. J. Biochem. *118*, 1104–1107.

Feng, J., Ito, M., Ichikawa, K., Isaka, N., Nishikawa, M., Hartshorne, D. J., and Nakano, T. (1999). Inhibitory phosphorylation site for Rho-associated kinase on smooth muscle myosin phosphatase. J. Biol. Chem. *274*, 37385–37390.

Firulli, A. B., Han, D., Kelly-Roloff, L., Koteliansky, V. E., Schwartz, S. M., Olson, E. N., and Miano, J. M. (1998). A comparative molecular analysis of four rat smooth muscle cell lines. In Vitro Cell Dev. Biol. Anim. *34*, 217–226.

Fredriksson, S., Gullberg, M., Jarvius, J., Olsson, C., Pietras, K., Gustafsdottir, S. M., Ostman, A., and Landegren, U. (2002). Protein detection using proximity-dependent DNA ligation assays. Nat. Biotechnol. *20*, 473–477.

Gimona, M., Kaverina, I., Resch, G. P., Vignal, E., and Burgstaller, G. (2003). Calponin repeats regulate actin filament stability and formation of podosomes in smooth muscle cells. Mol. Biol. Cell *14*, 2482–2491.

Given, A. M., Ogut, O., and Brozovich, F. V. (2007). MYPT1 mutants demonstrate the importance of aa 888-928 for the interaction with PKGIalpha. Am. J. Physiol. Cell Physiol. *292*, C432–C439.

Goswami, A., Burikhanov, R., de Thonel, A., Fujita, N., Goswami, M., Zhao, Y., Eriksson, J. E., Tsuruo, T., and Rangnekar, V. M. (2005). Binding and phosphorylation of par-4 by akt is essential for cancer cell survival. Mol. Cell *20*, 33–44.

Greenberg, J. I., *et al*. (2008). A role for VEGF as a negative regulator of pericyte function and vessel maturation. Nature *456*, 809–813.

Gurumurthy, S., Goswami, A., Vasudevan, K. M., and Rangnekar, V. M. (2005). Phosphorylation of Par-4 by protein kinase A is critical for apoptosis. Mol. Cell Biol. *25*, 1146–1161.

Hagerty, L., Weitzel, D. H., Chambers, J., Fortner, C. N., Brush, M. H., Loiselle, D., Hosoya, H., and Haystead, T. A. (2007). ROCK1 phosphorylates and activates zipper-interacting protein kinase. J. Biol. Chem. *282*, 4884–4893.

Huang, Q. Q., Fisher, S. A., and Brozovich, F. V. (2004). Unzipping the role of myosin light chain phosphatase in smooth muscle cell relaxation. J. Biol. Chem. *279*, 597–603.

Ito, M., Nakano, T., Erdodi, F., and Hartshorne, D. J. (2004). Myosin phosphatase: structure, regulation and function. Mol. Cell Biochem. *259*, 197–209.

Johnstone, R. W., *et al*. (1996). A novel repressor, par-4, modulates transcription and growth suppression functions of the Wilms' tumor suppressor WT1. Mol. Cell Biol. *16*, 6945–6956.

Joshi, J., *et al*. (2008). Par-4 inhibits Akt and suppresses Ras-induced lung tumorigenesis. EMBO J. *27*, 2181–2193.

Kawai, T., Akira, S., and Reed, J. C. (2003). ZIP kinase triggers apoptosis from nuclear PML oncogenic domains. Mol. Cell Biol. *23*, 6174–6186.

Khatri, J. J., Joyce, K. M., Brozovich, F. V., and Fisher, S. A. (2001). Role of myosin phosphatase isoforms in cGMP-mediated smooth muscle relaxation. J. Biol. Chem. *276*, 37250–37257.

Khromov, A., Choudhury, N., Stevenson, A. S., Somlyo, A. V., and Eto, M. (2009). Phosphorylation-dependent autoinhibition of myosin light chain phosphatase accounts for Ca2+ sensitization force of smooth muscle contraction. J. Biol. Chem. *284*, 21569–21579.

Kim, H. R., Gallant, C., Leavis, P. C., Gunst, S. J., and Morgan, K. G. (2008). Cytoskeletal remodeling in differentiated vascular smooth muscle is actin isoform dependent and stimulus dependent. Am. J. Physiol. Cell Physiol. *295*, C768–C778.

Kim, I., Leinweber, B. D., Morgalla, M., Butler, W. E., Seto, M., Sasaki, Y., Peterson, J. W., and Morgan, K. G. (2000). Thin and thick filament regulation of contractility in experimental cerebral vasospasm. Neurosurgery *46*, 440–446, 2000; discussion 446–447.

Kimes, B. W., and Brandt, B. L. (1976). Characterization of two putative smooth muscle cell lines from rat thoracic aorta. Exp. Cell Res. *98*, 349–366.

Kimura, K., *et al*. (1996). Regulation of myosin phosphatase by Rho and Rho-associated kinase (Rho-kinase). Science *273*, 245–248.

Kiss, E., Muranyi, A., Csortos, C., Gergely, P., Ito, M., Hartshorne, D. J., and Erdodi, F. (2002). Integrin-linked kinase phosphorylates the myosin phosphatase target subunit at the inhibitory site in platelet cytoskeleton. Biochem. J. *365*, 79–87.

Kögel, D., Plöttner, O., Landsberg, G., Christian, S., and Scheidtmann, K. H. (1998). Cloning and characterization of Dlk, a novel serine/threonine kinase that is tightly associated with chromatin and phosphorylates core histones. Oncogene *17*, 2645–2654.

Kohn, A. D., Takeuchi, F., and Roth, R. A. (1996). Akt, a pleckstrin homology domain containing kinase, is activated primarily by phosphorylation. J. Biol. Chem. *271*, 21920–21926.

Lai, J. M., Hsieh, C. L., and Chang, Z. F. (2003). Caspase activation during phorbol ester-induced apoptosis requires ROCK-dependent myosin-mediated contraction. J. Cell Sci. *116*, 3491–3501.

Larkin, M. A., *et al*. (2007). Clustal W and Clustal X version 2.0. Bioinformatics *23*, 2947–2948.

Lee, E., Hayes, D. B., Langsetmo, K., Sundberg, E. J., and Tao, T. C. (2007). Interactions between the leucine-zipper motif of cGMP-dependent protein kinase and the C-terminal region of the targeting subunit of myosin light chain phosphatase. J. Mol. Biol. *373*, 1198–1212.

Lee, T. J., Lee, J. T., Kim, S. H., Choi, Y. H., Song, K. S., Park, J. W., and Kwon, T. K. (2008). Overexpression of Par-4 enhances thapsigargin-induced apoptosis via down-regulation of XIAP and inactivation of Akt in human renal cancer cells. J. Cell Biochem. *103*, 358–368.

Leroy, I., de Thonel, A., Laurent, G., and Quillet-Mary, A. (2005). Protein kinase C zeta associates with death inducing signaling complex and regulates Fas ligand-induced apoptosis. Cell Signal. *17*, 1149–1157.

Lu, C., Chen, J. Q., Zhou, G. P., Wu, S. H., Guan, Y. F., and Yuan, C. S. (2008). Multimolecular complex of Par-4 and E2F1 binding to Smac promoter contributes to glutamate-induced apoptosis in human-bone mesenchymal stem cells. Nucleic Acids Res. *36*, 5021–5032.

MacDonald, J. A., Borman, M. A., Muranyi, A., Somlyo, A. V., Hartshorne, D. J., and Haystead, T. A. (2001). Identification of the endogenous smooth muscle myosin phosphatase-associated kinase. Proc. Natl. Acad. Sci. USA *98*, 2419–2424.

Matsui, T., Amano, M., Yamamoto, T., Chihara, K., Nakafuku, M., Ito, M., Nakano, T., Okawa, K., Iwamatsu, A., and Kaibuchi, K. (1996). Rho-associated kinase, a novel serine/threonine kinase, as a putative target for small GTP binding protein Rho. EMBO J. *15*, 2208–2216.

Mellberg, S., *et al*. (2009). Transcriptional profiling reveals a critical role for tyrosine phosphatase VE-PTP in regulation of VEGFR2 activity and endothelial cell morphogenesis. FASEB J.

Mizuno, Y., Isotani, E., Huang, J., Ding, H., Stull, J. T., and Kamm, K. E. (2008). Myosin light chain kinase activation and calcium sensitization in smooth muscle in vivo. Am. J. Physiol. Cell Physiol. *295*, C358–C364.

Muranyi, A., MacDonald, J. A., Deng, J. T., Wilson, D. P., Haystead, T. A., Walsh, M. P., Erdodi, F., Kiss, E., Wu, Y., and Hartshorne, D. J. (2002). Phosphorylation of the myosin phosphatase target subunit by integrin-linked kinase. Biochem. J. *366*, 211–216.

Murata-Hori, M., Suizu, F., Iwasaki, T., Kikuchi, A., and Hosoya, H. (1999). ZIP kinase identified as a novel myosin regulatory light chain kinase in HeLa cells. FEBS Lett. *451*, 81–84.

Nakamura, M., Ichikawa, K., Ito, M., Yamamori, B., Okinaka, T., Isaka, N., Yoshida, Y., Fujita, S., and Nakano, T. (1999). Effects of the phosphorylation of myosin phosphatase by cyclic GMP-dependent protein kinase. Cell Signal. *11*, 671–676.

Page, G., Kögel, D., Rangnekar, V., and Scheidtmann, K. H. (1999). Interaction partners of Dlk/ZIP kinase: co-expression of Dlk/ZIP kinase and Par-4 results in cytoplasmic retention and apoptosis. Oncogene *18*, 7265–7273.

Petrache, I., Verin, A. D., Crow, M. T., Birukova, A., Liu, F., and Garcia, J. G. (2001). Differential effect of MLC kinase in TNF-alpha-induced endothelial cell apoptosis and barrier dysfunction. Am. J. Physiol. Lung Cell Mol. Physiol. *280*, L1168–L1178.

Richard, D. J., Schumacher, V., Royer-Pokora, B., and Roberts, S. G. (2001). Par4 is a coactivator for a splice isoform-specific transcriptional activation domain in WT1. Genes Dev. *15*, 328–339.

Ridley, A. J., and Hall, A. (1992). The small GTP-binding protein rho regulates the assembly of focal adhesions and actin stress fibers in response to growth factors. Cell *70*, 389–399.

Sharma, A. K., Zhou, G. P., Kupferman, J., Surks, H. K., Christensen, E. N., Chou, J. J., Mendelsohn, M. E., and Rigby, A. C. (2008). Probing the interaction between the coiled coil leucine zipper of cGMP-dependent protein kinase Ialpha and the C terminus of the myosin binding subunit of the myosin light chain phosphatase. J. Biol. Chem. *283*, 32860–32869.

Shimizu, H., *et al*. (1994). Characterization of the myosin-binding subunit of smooth muscle myosin phosphatase. J. Biol. Chem. *269*, 30407–30411.

Shin, H. M., Je, H. D., Gallant, C., Tao, T. C., Hartshorne, D. J., Ito, M., and Morgan, K. G. (2002). Differential association and localization of myosin phosphatase subunits during agonist-induced signal transduction in smooth muscle. Circ. Res. *90*, 546–553.

Shirazi, A., Iizuka, K., Fadden, P., Mosse, C., Somlyo, A. P., Somlyo, A. V., and Haystead, T. A. (1994). Purification and characterization of the mammalian myosin light chain phosphatase holoenzyme. The differential effects of the holoenzyme and its subunits on smooth muscle. J. Biol. Chem. *269*, 31598–31606.

Söderberg, O., Leuchowius, K. J., Gullberg, M., Jarvius, M., Weibrecht, I., Larsson, L. G., and Landegren, U. (2008). Characterizing proteins and their interactions in cells and tissues using the in situ proximity ligation assay. Methods *45*, 227–232.

Surks, H. K., and Mendelsohn, M. E. (2003). Dimerization of cGMP-dependent protein kinase 1alpha and the myosin-binding subunit of myosin phosphatase: role of leucine zipper domains. Cell Signal. *15*, 937–944.

Surks, H. K., Mochizuki, N., Kasai, Y., Georgescu, S. P., Tang, K. M., Ito, M., Lincoln, T. M., and Mendelsohn, M. E. (1999). Regulation of myosin phosphatase by a specific interaction with cGMP-dependent protein kinase Ialpha. Science *286*, 1583–1587.

Vetterkind, S., Boosen, M., Scheidtmann, K. H., and Preuss, U. (2005a). Ectopic expression of Par-4 leads to induction of apoptosis in CNS tumor cell lines. Int. J. Oncol. *26*, 159–167.

Vetterkind, S., Illenberger, S., Kubicek, J., Boosen, M., Appel, S., Naim, H. Y., Scheidtmann, K. H., and Preuss, U. (2005b). Binding of Par-4 to the actin cytoskeleton is essential for Par-4/Dlk-mediated apoptosis. Exp. Cell Res. *305*, 392–408.

Vetterkind, S., and Morgan, K. G. (2009). The pro-apoptotic protein Par-4 facilitates vascular contractility by cytoskeletal targeting of Zipk. J. Cell Mol. Med. *13*, 887–895.

Wang, G., Silva, J., Krishnamurthy, K., Tran, E., Condie, B. G., and Bieberich, E. (2005). Direct binding to ceramide activates protein kinase Czeta before the formation of a pro-apoptotic complex with PAR-4 in differentiating stem cells. J. Biol. Chem. *280*, 26415–26424.

Wooldridge, A. A., MacDonald, J. A., Erdodi, F., Ma, C., Borman, M. A., Hartshorne, D. J., and Haystead, T. A. (2004). Smooth muscle phosphatase is regulated in vivo by exclusion of phosphorylation of threonine 696 of MYPT1 by phosphorylation of Serine 695 in response to cyclic nucleotides. J. Biol. Chem. *279*, 34496–34504.

Wooten, M. W., Seibenhener, M. L., Matthews, L. H., Zhou, G., and Coleman, E. S. (1996). Modulation of zeta-protein kinase C by cyclic AMP in PC12 cells occurs through phosphorylation by protein kinase A. J. Neurochem. *67*, 1023–1031.